NANO LETTERS

Letter

pubs.acs.org/NanoLett

Structure of a Peptide Adsorbed on Graphene and Graphite

Jyoti Katoch,[†,‡] Sang Nyon Kim,[§] Zhifeng Kuang,[§] Barry L. Farmer,[§] Rajesh R. Naik,[§] Suren A. Tatulian,[†] and Masa Ishigami*[,†,‡]

[†]Department of Physics, University of Central Florida, Orlando, Florida 32816-2385, United States

[‡]Nanoscience Technology Center, University of Central Florida, Orlando, Florida 32816-2385, United States

[§]Materials and Manufacturing Directorate, Air Force Research Laboratory, Wright-Patterson Air Force Base, Ohio 45433, United States

ABSTRACT: Noncovalent functionalization of graphene using peptides is a promising method for producing novel sensors with high sensitivity and selectivity. Here we perform atomic force microscopy, Raman spectroscopy, infrared spectroscopy, and molecular dynamics simulations to investigate peptide-binding behavior to graphene and graphite. We studied a dodecamer peptide identified with phage display to possess affinity for graphite. Optical spectroscopy reveals that the peptide forms secondary structures both in powder form and in an aqueous medium. The dominant structure in the powder form is α-helix, which undergoes a transition to a distorted helical structure in aqueous solution. The peptide forms a complex reticular structure upon adsorption on graphene and graphite, having a helical conformation different from α-helix due to its interaction with the surface. Our observation is consistent with our molecular dynamics calculations, and our study paves the way for rational functionalization of graphene using biomolecules with defined structures and, therefore, functionalities.

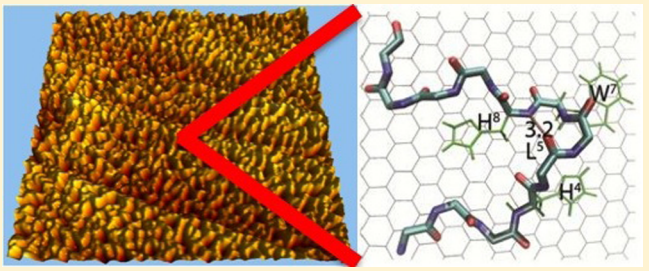

KEYWORDS: *Graphene, functionalization, phage displayed peptides, atomic force microscopy, Raman spectroscopy, infrared spectroscopy, molecular dynamics simulation*

Graphene sheet, an individual layer of graphite, is a semimetal with unusual physical properties.[1,2] Graphene possesses no dangling bonds except at the edges, and their well-ordered chemical structure renders chemical interactions with the surrounding environment more predictable. In addition, transport properties of graphene are characterized by extraordinary field effect mobility even at room temperature.[3] High field effect mobility renders graphene sheets to be highly sensitive to their environment, making them ideal for sensing applications.

Graphene-based field effect transistors show a sensitive, yet nonselective, response to various analytes,[4] and it is now widely accepted that selectivity, necessary for any sensors, must be imparted by functionalization. Since high sensitivity relies on high mobility, functionalization must leave the transport property of graphene unaffected. Noncovalent functionalization is ideal as it does not generate atomic-scale defects, which are extremely disruptive.[5−8]

One of many promising noncovalent functionalization methods seeks to mimic and exploit the molecular recognition property of peptides found in biology[9] to impart selectivity for a wide variety of analytes. Resolving peptide structures is fundamentally important to this biomimetic approach because properties of peptides are sensitively influenced by their structures. Although the binding of peptides has been visualized using atomic force microscopy (AFM) on nanotubes[10] and graphene,[11,12] AFM cannot be used to resolve the peptide structure. Previous studies have utilized molecular dynamics (MD) simulations[13,14] to infer the structure of bound peptides,[10−12] but additional experimental studies are needed to confirm the validity of these calculations.

Here in this paper, we have performed AFM, Raman, and Fourier transform infrared (FTIR) spectroscopy to study the structure of peptides bound to graphene and graphite. This integrated strategy enabled gathering of the fingerprint signatures of the peptide, which contains information on its secondary structure. Our experimental results confirm the behavior of the peptide calculated in MD simulations. Therefore, the results demonstrate that MD simulations can be relevant for predicting the behavior of peptide-functional groups on graphene and identifying proper functional groups for various analytes.

Graphene sheets were produced using the mechanical exfoliation method,[15] and the layer thicknesses were confirmed using Raman spectroscopy.[16] Grade II HOPG used for this study was purchased from Structure Probe, Inc. The dodecamer peptide, GAMHLPWHMGTL, was synthesized by Peptide 2.0 Inc. (Chantilly, VA) at a purity of 99.39%, verified by high performance liquid chromatography. The peptide was previously identified to bind to HOPG using phage display.[11]

Received: January 23, 2012
Revised: March 20, 2012
Published: April 3, 2012

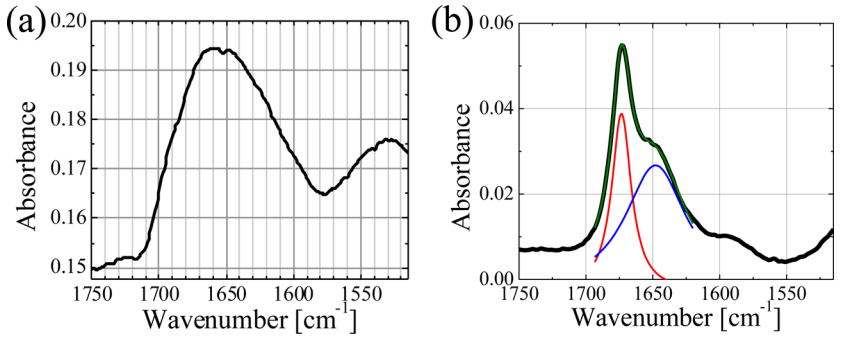

Figure 1. (a) Infrared spectrum of GBP in powder form, showing both amide I and amide II bands. (b) Infrared spectrum of GBP in D_2O, showing the amide I band. Red and blue curves are obtained by fitting two Lorentzian functions to the experimental data. The peaks are located at 1673 and 1648 cm^{-1}. The green curve is the result of sum of these functions.

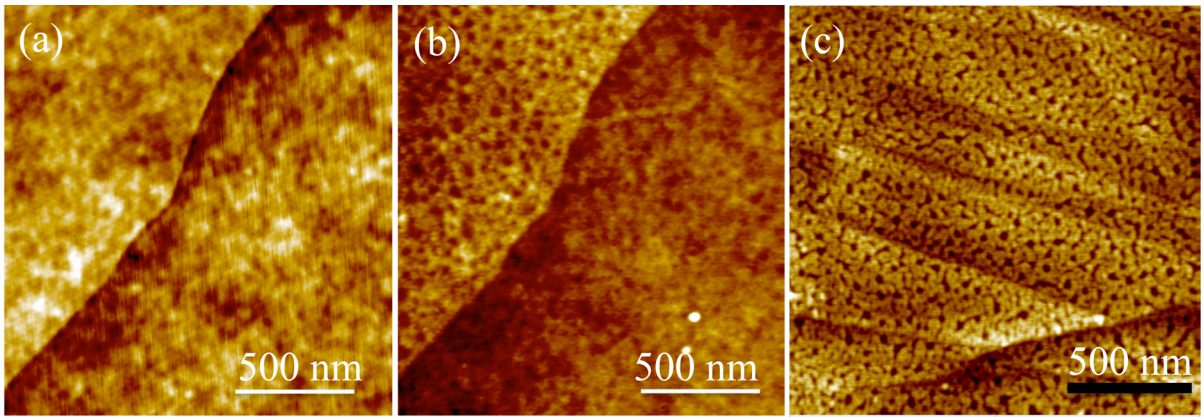

Figure 2. AFM topographic image of graphene (a) before and (b) after incubation with the peptide. (c) Topographic AFM image of HOPG incubated with the peptide.

This graphene/graphite binding peptide (GBP) was then dissolved in an aqueous buffer (100 mM Tris-HCl, pH 7.5) at a concentration of 200 μg/mL. Graphene sheets and HOPG were immersed in the GBP solution for 10 min at room temperature, washed with deionized water, and blown dry with N_2 gas prior to analysis. A Digital Instruments 5000 AFM, operating in ambient environment, was used for imaging. Raman spectra were acquired using a Renishaw Raman spectrometer with a 532 nm laser (5% laser power, exposure time of 50 s, and 4 accumulations). FTIR and attenuated total reflectance (ATR)-FTIR measurements were acquired using a Vector 22 Fourier transform infrared spectrometer (Bruker Optics, Billerica, MA), equipped with a liquid nitrogen-cooled Hg−Cd−Te detector. FTIR of the lyophilized peptide powder was measured by pressing the powder between two CaF_2 windows, using the spectrum of the CaF_2 window as reference. FTIR of the peptide in a D_2O-based buffer (150 mM NaCl, 40 mM HEPES, pH 7.2) was measured using a 25 μm spacer between the windows, using a buffer solution as reference. ATR-FTIR spectra were measured by mechanically contacting HOPG with a 1 mm thick germanium internal reflection plate (Spectral Systems, Irvington, NY) at 20 ± 1 °C. Each spectrum was the average of 1000 scans, at 2 cm^{-1} nominal resolution. The reference spectra were measured using a bare germanium plate. Atmospheric humidity was monitored by collecting spectra at various times, using the bare CaF_2 window or the germanium plate, and were used for clearing the sample spectra of signals generated by residual humidity.

The FTIR spectrum of the GBP in the powder form displays a relatively broad amide I band with a peak in the 1660−1650 cm^{-1} region as well as an amide II band around 1530 cm^{-1}, as shown in Figure 1a. The peak position of the dry peptide indicates an α-helical secondary structure.[17−20] When dissolved in a D_2O-based buffer, the GBP exhibits a dominant amide I peak at 1673 cm^{-1} accompanied by a smaller peak at 1648 cm^{-1}, as shown in Figure 1b. The amide II band disappears because of amide NH-to-ND conversion. Higher amide I frequencies in D_2O can be generated by various secondary structures, such as α_{II}-helix, 3_{10}-helix, reverse turns, or antiparallel β-sheet.[17−20] The latter can be excluded because the antiparallel β-sheet structure generates a strong component around 1635 cm^{-1} and a weaker component around 1685 cm^{-1}.[18] While the FTIR data do not allow distinction between α_{II}-helix, 3_{10}-helix, or turn structures, the observed amide I spectra strongly suggest that at least a part of the secondary structure of the peptide changes from α-helix to another helical or turn structure upon exposure to an aqueous medium.

Incubation of graphene with the peptide results in formation of a meshlike layer as shown in Figure 2. This mesh layer is found on all imaged areas showing that the adsorbed layer uniformly coats graphene. Silicon oxide surface appears unaffected by incubation, indicating that the adsorption only occurs specifically on graphene. The height difference to the substrate, measured by using height histograms, increases from 0.46 ± 0.33 to 1.45 ± 0.54 nm upon incubation, suggesting that the adsorbed layer is 0.99 ± 0.63 nm thick. This thickness is similar to that observed when a dodecamer peptide was

dx.doi.org/10.1021/nl300286k | Nano Lett. 2012, 12, 2342−2346

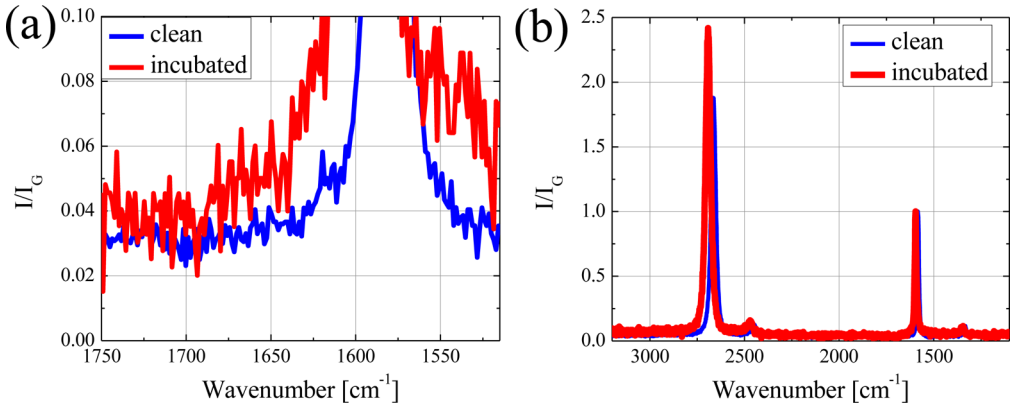

Figure 3. Raman spectroscopy of graphene before and after incubation with the peptide (a) between 1750 and 1525 cm^{-1} and (b) 3200 and 1100 cm^{-1}. Intensities are normalized with respect to the intensity of the G band.

adsorbed onto carbon nanotubes.[10] Graphene and graphite possess same surface chemical structures, and the interactions of these surfaces with peptides are expected to be similar. The AFM image of HOPG incubated with the GBP is shown in Figure 2c. A similar meshlike layer appears on the HOPG surface upon incubation. Furthermore, the thickness of the adsorbed layer on HOPG is measured to be 1.10 ± 0.45 nm,[21] indistinguishable from the thickness of the peptide layer on graphene. As such, these AFM images show that the identical adsorbed layer is formed on graphene and HOPG, as expected. The adsorbed layer on HOPG is used to obtain enhanced optical spectra below.

Figure 3a compares Raman spectra of graphene before and after incubation with the peptide. Bare graphene exhibits a strong Raman signal around 1580 cm^{-1} due to its G band.[16] Incubation with the peptide produces increased signals at both 1700−1600 and 1570−1520 cm^{-1} regions, consistent with the amide I and amide II modes of the peptide. The peak near 1350 cm^{-1}, corresponding to the D-band, does not increase in intensity as shown in Figure 3b. The I_D/I_G ratio is proportional to the defect density,[22] and as such, the spectra show that absorption of the peptide does not damage the graphene lattice, consistent with the expected noncovalent interaction between graphene and the peptide.

ATR-FTIR spectroscopy was used to increase the signal-to-noise ratio to further analyze the nature of the adsorbed layer. Spectra display absorption bands peaking near 1670 and 1550−1540 cm^{-1} for the adsorbed peptide layer, as shown in Figure 4. The peak at 1580 cm^{-1} is due to the G band in graphite.[16] The spectral locations of 1670 and 1550−1540 cm^{-1} bands due to the adsorbed layer are consistent with the amide I and II bands

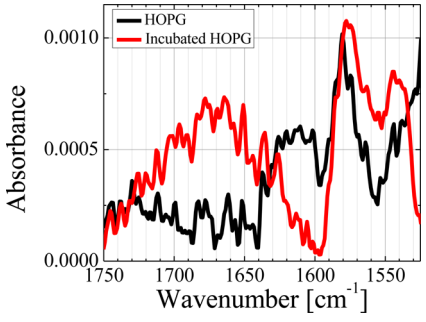

Figure 4. ATR-FTIR spectra of HOPG before and after incubation with the peptide.

and represent the first spectroscopic evidence that the adsorbed layer is indeed the GBP. The enhanced signal also reveals more details of the nature of the adsorbed peptide. The amide I band is blue-shifted to around 1670 cm^{-1}, compared to 1660−1650 cm^{-1} for the peptide in the powder form shown in Figure 1a. Normally, the α-helical amide I mode of peptides in aqueous media is around 1655−1650 cm^{-1}.[17,23,24] The amide I band of the 3_{10}-helical structure is typically at 1665 cm^{-1},[18,25] and the adsorbed layer may be conformed to a 3_{10}-helix structure. In addition, since the main contribution to the amide I mode comes from the peptide backbone C═O stretching vibration, higher amide I wavenumber (frequency) may also indicate stronger C═O bonds, which corresponds to weaker intra- or intermolecular hydrogen bonding. Blue-shifted amide I bands observed for α_{II}-helical structures in proteins and model polypeptides have also been attributed to weakened helical hydrogen bonding.[26−30] Therefore, the increased amide I wavenumber of the adsorbed peptide indicates that the peptide−graphite/graphene interaction induces the GBP to conform to a 3_{10}- or α_{II}-helix structure.

To understand the observed structural changes of the GBP at the atomic level, we utilized the MD simulation approach using the AMBER ff99SB force field.[31] The five most probable initial structures of the GBP were predicted using I-TASSER software.[32] Five structures were first refined by performing MD simulations in vacuum. After 200 ns simulations, the radius of gyration of structures converged. The conformation of the native GBP at the lowest potential energy exhibits a highly ordered α-helix structure by forming $i + 4 \rightarrow i$ hydrogen bonding between H^4−H^8 and L^5−M^9 pairs as shown in Figure 5a. This predicted helical structure is in agreement with our FTIR data on the GBP powder. Placing the peptide in the center of a water box with 1.2 nm TIP3P water layer in each direction, five independent molecular dynamics simulations were performed for 90 ns (40 and 50 ns in ntv and npt configuration, respectively) using various initial velocity. In contrast to the ordered helical structure in powder form, strong hydrophilicity of the histidine residues destabilizes the α-helical structure and transforms the GBP to a distorted α-helical structure as shown in Figure 5b. The distorted GBP resembles 3_{10}-helix by forming $i + 3 \rightarrow i$ hydrogen bonding between H^4−W^7 and L^5−H^8 pairs as shown. Such transformation in the aqueous environment is consistent with our FTIR spectra. When molecular dynamics simulations were performed on five different systems consisting of the peptide and 5 × 5 nm graphene sheet terminated with hydrogen at its edges as

dx.doi.org/10.1021/nl300286k | Nano Lett. 2012, 12, 2342−2346

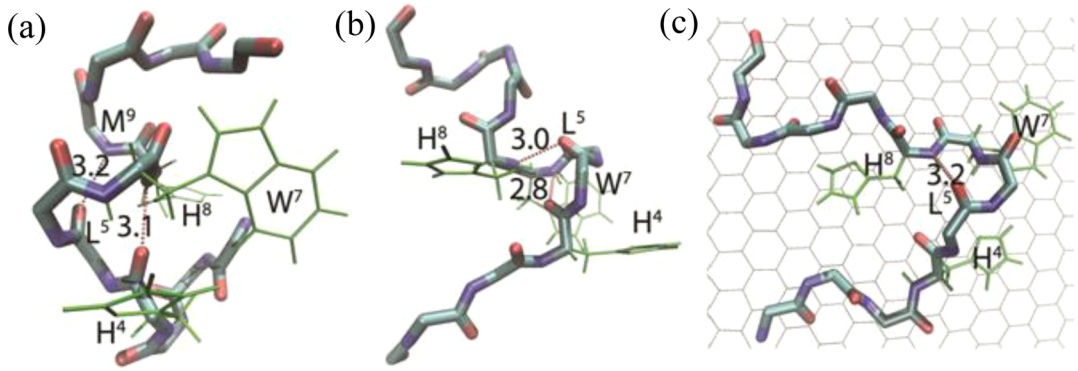

Figure 5. Molecular dynamics based structure of GAM peptide (a) in vacuum, (b) in water, and (c) on a 5 nm × 5 nm graphene sheet. For clarity, only part of the graphene sheet is displayed.

described previously,[12] the results converged after 40 ns and the GBP was observed to conform to graphene surface as shown in Figure 5c with an interaction energy of −106 ± 5 kcal/mol. The indole and imidazole side chains of tryptophan and histidine residues appear to parallel to the graphene sheet, distorting the helical structure and weakening the hydrogen bonding. Such calculated behavior is also consistent with our ATR-FTIR measurement of the adsorbed GBP on HOPG. Finally, to elucidate the binding mechanism, the representative structure as shown in Figure 5c was mutated and minimized. Tryptophan, histidine-4, or histidine-8 was substituted with alanine. The minimized interaction energies for the wild peptide, tryptophan to alanine, histidine-4 to alanine, and histidine-8 to alanine are −126 ± 0.2, −112 ± 0.2, −115 ± 0.4, and −123 ± 0.1 kcal/mol, respectively. These interaction energies imply that tryptophan is needed for efficient binding to graphene.

In conclusion, our vibrational spectroscopy and atomic force microscopy data show that the GBP, identified earlier using phage display,[11] binds noncovalently to graphene and HOPG. Direct transmission FTIR spectra indicate that the peptide forms secondary structures both in powder form and in an aqueous medium. The dominant structure in the powder form is α-helix, which undergoes a transition to a distorted helical structure in aqueous solution. AFM images indicate that identical adsorbed layers are formed upon incubation on graphene and HOPG. Raman spectra show that incubation does not cause any chemical perturbation to graphene, implying that the peptide functionalizes graphene noncovalently as expected. The ATR-FTIR spectra of the adsorbed layer on HOPG indicate that the GBP is in a helical conformation, which is different from α-helix, due to its interaction with the surface. Our result thus provides new insights into how the peptide interacts with the graphene surface and serves as an important experimental confirmation of MD simulations, which are essential in designing peptide−graphene sensors with high sensitivity and selectivity. Finally, the result also shows that our approach can be useful for further studies of a wide variety of graphene-binding peptides.

AUTHOR INFORMATION

Notes

The authors declare no competing financial interest.

ACKNOWLEDGMENTS

This work is based on research supported by the National Science Foundation under Grant No. 0955625 (J.K. and M.I.), by the Summer Faculty Fellowship Program of the Air Force Office of Scientific Research (M.I.), and by the Air Force Office of Scientific Research (R.N.).

REFERENCES

(1) Geim, A. K. Graphene: Status and Prospects. *Science* **2009**, *324* (5934), 1530−1534.
(2) Geim, A. K.; Novoselov, K. S. The Rise of Graphene. *Nat. Mater.* **2007**, *6* (3), 183.
(3) Newaz, A. K. M.; Puzyrev, Y. S.; Wang, B.; Pantelides, S. T.; Bolotin, K. I. Probing charge scattering mechanisms in suspended graphene by varying its dielectric environment. *Nature Communications* **2012**, *3*, 734.
(4) Dan, Y. P.; Lu, Y.; Kybert, N. J.; Luo, Z. T.; Johnson, A. T. C. Intrinsic Response of Graphene Vapor Sensors. *Nano Lett.* **2009**, *9* (4), 1472−1475.
(5) Ostrovsky, P. M.; Gornyi, I. V.; Mirlin, A. D. Electron Transport in Disordered Graphene. *Phys. Rev. B* **2006**, *74*, 235443.
(6) Titov, M.; Ostrovsky, P. M.; Gornyi, I. V.; Schuessler, A.; Mirlin, A. D. Charge Transport in Graphene with Resonant Scatterers. *Phys. Rev. Lett.* **2010**, *104* (7), 076802.
(7) Stauber, T.; Peres, N. M. R.; Guinea, F. Electronic Transport in Graphene: A Semiclassical Approach Including Midgap States. *Phys. Rev. B* **2007**, *76*, 205423.
(8) Wehling, T. O.; Katsnelson, M. I.; Lichtenstein, A. I. Impurities on Graphene: Midgap States and Migration Barriers. *Phys. Rev. B* **2009**, *80* (8), 085428.
(9) Sarikaya, M.; Tamerler, C.; Jen, A. K. Y.; Schulten, K.; Baneyx, F. Molecular Biomimetics: Nanotechnology through Biology. *Nat. Mater.* **2003**, *2* (9), 577−585.
(10) Kuang, Z.; Kim, S. N.; Crookes-Goodson, W. J.; Farmer, B. L.; Naik, R. R. Biomimetic Chemosensor: Designing Peptide Recognition Elements for Surface Functionalization of Carbon Nanotube Field Effect Transistors. *ACS Nano* **2009**, *4* (1), 452.
(11) Cui, Y.; Kim, S. N.; Jones, S. E.; Wissler, L. L.; Naik, R. R.; McAlpine, M. C. Chemical Functionalization of Graphene Enabled by Phage Displayed Peptides. *Nano Lett.* **2010**, *10* (11), 4559−4565.
(12) Kim, S.; Kuang, N. Z.; Slocik, J. M.; Jones, S. E.; Cui, Y.; Farmer, B. L.; McAlpine, M. C.; Naik, R. R. Preferential Binding of Peptides to Graphene Edges and Planes. *J. Am. Chem. Soc.* **2011**, *133*, 14480.
(13) Daggett, V. Protein Folding-Simulation. *Chem. Rev.* **2006**, *106*, 1898.
(14) Gnanakaran, S.; Nymeyer, H.; Portman, J.; Sanbonmatsu, K. Y.; Garcia, A. E. Peptide Folding Simulation. *Curr. Opin. Struct. Biol.* **2003**, *13*, 168.

(15) Novoselov, K. S.; Jiang, D.; Schedin, F.; Booth, T. J.; Khotkevich, V. V.; Morozov, S.; Geim, A. K. Two-Dimensional Atomic Crystals. *Proc. Natl. Acad. Sci. U. S. A.* **2005**, *102* (30), 10451.
(16) Dresselhaus, M. S.; Jorio, A.; Hofmann, M.; Dresselhaus, G.; Saito, R. Perspectives on Carbon Nanotubes and Graphene Raman Spectroscopy. *Nano Lett.* **2010**, *10*, 751.
(17) Tatulian, S. A. Attenuated Total Reflection Fouier Transform Infrared Spectroscopy: A Method of Choice for Studying Membrane Proteins and Lipids. *Biochemistry* **2003**, *42*, 11898−11907.
(18) Krimm, S.; Bandekar, J. Vibrational Spectroscopy and Conformation of Peptides, Polypeptides, and Proteins. *Adv. Protein Chem.* **1986**, *38*, 181−364.
(19) Surewicz, W. K.; Mantsch, H. H.; Chapman, D. Determination of Protein Secondary Structure by Fourier Transform Infrared Spectroscopy: A Critical Assessment. *Biochemistry* **1993**, *32*, 389−394.
(20) Arrondo, J. L. R.; Goni, F. M. Structure and Dynamics of Membrane Proteins As Studied by Infrared Spectroscopy. *Prog. Biophys. Mol. Biol.* **1999**, *72*, 367−405.
(21) Measured at the locations where the flat HOPG is visible.
(22) Lucchese, M. M.; Stavale, F.; Ferreira, E. H. M.; Vilani, C.; Moutinho, M. V. O.; Capaz, R. B.; Achete, C. A.; Jorio, A. Quantifying Ion-Induced Defects and Raman Relaxation Length in Graphene. *Carbon* **2010**, *48* (5), 1592−1597.
(23) Haris, P. I.; Chapman, D. The Conformational Analysis of Peptides Using Fourier Transform IR Spectroscopy. *Biopolymers (Pept. Sci.)* **1995**, *37*, 251.
(24) Jackson, M.; Mantsch, H. H. The Use and Misuse of FTIR Spectroscopy in the Determination of Protein Structure. *Crit. Rev. Biochem. Mol. Biol.* **1995**, *30* (2), 95−120.
(25) Kennedy, D. F.; Crisma, M.; Toniolo, C.; Chapman, D. Studies of Peptides Forming 3_{10}- and Alpha Helices and Beta-Bend Ribbon Structures in Organic Solution and in Model Biomembranes by Fourier Transform Infrared Spectroscopy. *Biochemistry* **1991**, *30*, 6541.
(26) Cladera, J.; Sabes, M.; Padros, E. Fourier Transform Infrared Analysis of Bacteriorhodopsin Secondary Structure. *Biochemistry* **1992**, *31* (49), 12363.
(27) Dwevedi, A. M.; Krimm, S. Vibrational Analysis of Peptides, Polypeptides, and Proteins. *Biopolymers (Pept. Sci.)* **1984**, *23*, 923.
(28) Krimm, S.; Dwevedi, A. M. Infrared Spectrum of the Purple Membrane: Clue to a Proton Conduction Mechanism? *Science* **1982**, *216*, 407.
(29) Nemethy, G.; Phillips, D. C.; Leach, S. J.; Scheraga, H. A. A Second Right-Handed Helical Structure with the Parameters of the Pauling-Coarey Alpha-Helix. *Nature* **1967**, *214*, 363.
(30) Torres, J.; Sepulcre, F.; Padros, E. Conformational Changes in Bacteriorhodopsin Associated with Protein-Protein Interactions: A Functional Alpha I-Alpha II Helix Switch? *Biochemistry* **1995**, *34*, 16320.
(31) Case, D. A.; Cheatham, T. E., III; Darden, T.; Gohlke, H.; Luo, R.; Merz, K. M., Jr.; Onufriev, A.; Simmerling, C.; Wang, B.; Woods, R. J. The Amber Biomolecular Simulation Programs. *J. Comput. Chem.* **2005**, *26* (16), 1668−1688.
(32) http://zhanglab.ccmb.med.umich.edu/I-TASSER.